Variation of transverse forces on nearby shield tunnel caused by foundation pits excavation

Gang WEI
Department of Civil Engineering, Zhejiang University City College, Hangzhou, Zhejiang 310015, China

Xin-hai ZHANG
College of Civil Engineering and Architecture, Zhejiang University, Hangzhou, Zhejiang 310058, China

Xin-bei LIN
Department of Civil Engineering, Zhejiang University City College, Hangzhou, Zhejiang 310015, China

Xin-xin HUA
CREEC East China Survey and Design Co., Ltd., Hangzhou, Zhejiang 310004, China

Variation of transverse forces on nearby shield tunnel caused by foundation pits excavation

WEI Gang[1],   ZHANG Xin-hai[2],   LIN Xin-bei[1],   HUA Xin-xin[3]

1. Department of Civil Engineering, Zhejiang University City College, Hangzhou, Zhejiang 310015, China

2. College of Civil Engineering and Architecture, Zhejiang University, Hangzhou, Zhejiang 310058, China

3. CREEC East China Survey and Design Co., Ltd., Hangzhou, Zhejiang 310004, China

Abstract: In order to study the influence of excavation near shield tunnels on the force of tunnel segments, the mechanism of surrounding pressure change on tunnels caused by nearby excavation is studied. A model of additional confining pressure redistribution is proposed which can describe the process of force-displacement-rebalancing of tunnels, and the calculation formula of additional confining pressure is deduced. The internal force of lining under the corresponding confining pressure is calculated by using the modified routine method. The influence of foundation pit excavation on the confining pressure and internal force of shield tunnels is studied based on the analysis of a practical engineering example, and the influencing factors are analyzed. The analysis results show that confining pressure of the tunnel before excavation presents a "bell shape" distribution. After excavation, the confining pressure on both sides of the tunnel decreases, and the confining pressure on the excavation side decreases more. The excavation of the foundation pit increases the positive and negative bending moments and the positive and negative shear forces of the nearby tunnel, and decreases the axial forces of the arch top and the arch bottom. With the increase of the stress release coefficient of the side wall of the foundation pit, both the absolute values of the additional confining pressure and of the additional bending moment will increase, and the response of bending moment to unloading of foundation pit excavation is more obvious. Shallow shield tunnel is more sensitive to the influence of the excavation of side foundation pit, and the influence of excavation of side foundation pit will decrease obviously when the burial depth of the tunnel is greater than that of the foundation pit excavation. With the increase of the distance between the foundation pit and the nearby tunnel, the influence of the foundation pit excavation on the tunnel will also be reduced.

Keywords: foundation pits excavation; nearby shield tunnel; transverse force; redistribution of confining pressure; modified routine method

1 Introduction

The fast development of urban rail transit in China has significantly increased the demands for utilization of underground spaces, which inevitably involves carrying out excavation in the vicinity of operating shield tunnels. For example, the deep foundation pit near People's Square Station of Hangzhou Metro Line 2 is distanced from the operating shield tunnel by 9.5 m only[1]; the foundation pit near the Cross River Shield Tunnel on Tibet South Road in Shanghai is 9.7 m to the nearby tunnel[2]; the foundation pit on the south side of Nanjing West Road Station-Jing'an Temple Station of Shanghai Rail Transit Line 2 is 8m to the shield tunnel [3]. Actually, it is not uncommon to carry out such foundation pit excavation works rightly beside existing tunnels. As such, the unloading effect of the side wall of the foundation pit will be transmitted to the neighbouring shield tunnel through the soil mass deformation, which will cause surcharge loading on the tunnel structure and destroy the force balance of the segment structure, leading to tunnel deformation, and even further damage. In order to ensure the track lines in operational condition, rigorous requirements given by relevant regulations have to be met for

tunnel deformation control[4]. Therefore, the study of the influence of foundation pit excavation on the neighboring shield tunnel will provide useful guidance for the underground engineering practices.

With respect to the problems as mentioned above, some researches have been carried out both domestically and internationally. The research methods include statistical analysis of measured data[5–6], numerical simulation[7–8], theoretical calculation[9–10], and centrifuge model test[11]. Most of them are focused on the longitudinal deformation of the neighbouring tunnel caused by the excavation of the foundation pit, and there are few studies on the change of the lining confining pressure and the lateral deformation. Zheng et al.[7] used a two-dimensional finite element model to analyze the cross-section displacements of tunnels at different positions under different deformation modes and deformation amounts of the envelope structure, and divided the impact zone. Hu et al. [8] obtained the change of the tunnel confining pressure caused by the excavation of the foundation pit by numerical simulation, and calculated the internal force of the segment. The researches on the lateral force and deformation of tunnels are mostly numerical simulations, which are often insufficient to provide

theoretical solution of the lining confining pressure changes that provide the basis for full-scale shield segment loading tests. Therefore, it is urgent to explore the theoretical solution of the tunnel confining pressure caused by the excavation of the foundation pit by analytical method, and then to study the force of the tunnel structure to provide basis for the safety evaluation of subway tunnel operation.

In this paper, based on the unloading model of foundation pit excavation, the Mindlin's solution is used to calculate the additional soil stress caused by the foundation pit excavation, and to obtain the lateral surcharge load distribution of the tunnel. Then, the mechanism of tunnel confining pressure caused by the excavation is analyzed. An additional confining pressure redistribution model that can describe the lateral displacement rebalance of the tunnel is proposed, and the calculation equation of additional confining pressure is derived. The initial confining pressure of the tunnel is obtained based on the load combinations of normal working conditions when the foundation pit is not yet constructed. The final confining pressure of the tunnel after excavation is obtained by superimposing the additional confining pressure obtained by the model in this paper. By using the Shield Tunnel Design and Analysis software of GeoFBA, the modified routine method is used to calculate the internal force of the tunnel lining under the corresponding confining pressure. Based on actual engineering examples, the effect of excavation on the confining pressure and internal force of the tunnel lining is studied. The influence factors such as the stress release coefficient of the side wall, the distance between the foundation pit and the tunnel, and the depth of the tunnel are analyzed.

2 Analysis procedures

2.1 Mechanical model for calculation

The theoretical calculation model for excavation of rectangular foundation pit beside shield tunnel is shown in Fig.1. At first, a coordinate system at the center o of the ground foundation pit is established, and the x-axis and y-axis are perpendicular and parallel to the tunnel axis, respectively. The positive z-axis direction is vertically downward. The size of the excavation along the y-axis is L, and B along the x-axis, and the depth of the excavation is d. The horizontal distance between the tunnel axis and the center of the foundation pit is a, the outer diameter of the shield tunnel is D, the buried depth of the tunnel axis is h, and the minimum net distance from the foundation pit envelope to the tunnel is $s(s = a - B/2 - D/2)$. The insertion depth of the retaining structure below the bottom of the foundation pit is d_0, and the total height of the retaining structure of the foundation pit is H ($H = d + d_0$). Therefore, the coordinate of any point on the tunnel axis is (a, l, h), where l is the horizontal distance between the calculated point on the tunnel along the y-axis and the excavation center of the foundation pit. As shown in Fig.1 (a), the four side walls of the foundation pit are numbered as ①, ②, ③, and ④. The side walls ① and ③ are parallel to the tunnel axis, and the side wall ① is located beside the tunnel. The side walls ② and ④ are perpendicular to the tunnel axis.

(a) Flat figure

(b) Profile figure
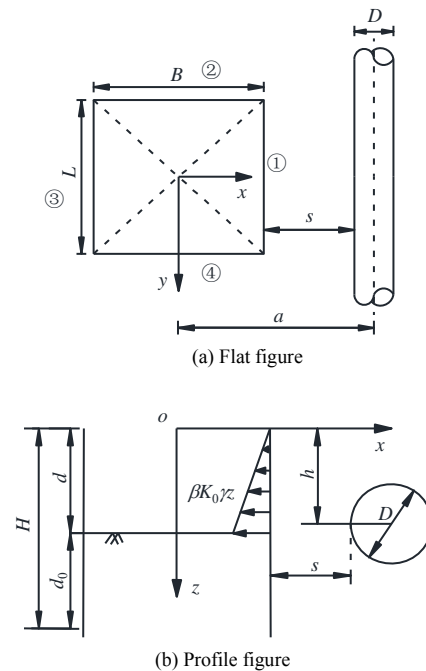
Fig.1 Schematic diagram of the relationship between the excavated foundation pit and the nearby shield tunnel

For foundation pits with cantilever-type retaining structures, the retaining structure must be inserted at a certain depth from the bottom of the pit, the unloading effect at the bottom of the pit will not directly affect the soil layer outside the pit under the shelter of the retaining structure. Wei et al.[12] calculated the equivalent load at the bottom plane of the retaining structure by using the residual stress method and considering the side frictional resistance of retaining structure of the pit bottom, followed by calculating the additional stress of the soil caused by the equivalent load. According to the results of this method, the unloading effect of the bottom of the pit on the nearby tunnel under the sheltering effect of the retaining structure below the bottom of the pit has a small impact on the nearby tunnels, which is negligible compared with the direct effect of side wall unloading. Zhang et al.[10] superposed the unloading effects of all the side walls of the foundation pit when calculating the surcharge load of the nearby tunnel caused by the excavation. According to their study, the side wall ③ of the foundation pit and the tunnel are separated by the excavated foundation pit, and the unloading effect of the side wall ③ will not be transmitted to the tunnel. Therefore, only the unloading effects of the side wall ① and the side walls ② and ④ are considered in the calculation of the surcharge loads of the tunnel.

2.2 Effect of foundation pit unloading on the tunnel confining pressure

2.2.1 Surcharge loads on tunnel caused by unloading of the side walls of the foundation pit

First, it is assumed that the influence of the tunnel structure will not be considered herein. According to the Mindlin's solution[13], applying a unit force to (x_1, y_1, z_1) along the x-axis in a semi-infinite elastic body, the additional stress in the x-axis at the point (x, y, z) is

$$\sigma_{xx}(x,y,z,x_1,y_1,z_1) = \frac{(x-x_1)}{8\pi(1-\mu)}\left\{\frac{1-2\mu}{M^3} - \right.$$
$$\frac{(1-2\mu)(5-4\mu)}{N^3} + \frac{3(3-4\mu)(x-x_1)^2}{N^5} +$$
$$\frac{4(1-\mu)(1-2\mu)}{N(N+z+z_1)^2}\left[3 - \frac{(x-x_1)^2(3N+z+z_1)}{N^2(N+z+z_1)}\right] + \quad (1)$$
$$\frac{3(x-x_1)^2}{M^5} - \frac{6z_1}{N^5}\cdot$$
$$\left.\left[3z_1 - (3-2\mu)(z+z_1) + \frac{5(x-x_1)^2 z}{N^2}\right]\right\}$$

The additional stress in the z direction is

$$\sigma_{zx}(x,y,z,x_1,y_1,z_1) = \frac{(x-x_1)}{8\pi(1-\mu)}\left\{\frac{-1+2\mu}{M^3} + \frac{1-2\mu}{N^3} + \right.$$
$$\frac{3(z-z_1)^2}{M^5} + \frac{3(3-4\mu)(z+z_1)^2}{N^5} - \quad (2)$$
$$\left.\frac{6z_1}{N^5}\left[z_1 + (1-2\mu)(z+z_1) + \frac{5z(z+z_1)^2}{N^2}\right]\right\}$$

where μ is Poisson's ratio of soil;

$$M = \sqrt{(x-x_1)^2 + (y-y_1)^2 + (z-z_1)^2} \;;$$
$$N = \sqrt{(x-x_1)^2 + (y-y_1)^2 + (z+z_1)^2} \;。$$

Applying an unit force to (x_1, y_1, z_1) along the y-axis in a semi-infinite elastic body, the additional stress along the x-axis generated at the point (x, y, z) is

$$\sigma_{xy}(x,y,z,x_1,y_1,z_1) = \frac{(y-y_1)}{8\pi(1-\mu)}\left\{\frac{1-2\mu}{M^3} - \right.$$
$$\frac{(1-2\mu)(5-4\mu)}{N^3} + \frac{3(3-4\mu)(y-y_1)^2}{N^5} +$$
$$\frac{4(1-\mu)(1-2\mu)}{N(N+z+z_1)^2}\left[3 - \frac{(y-y_1)^2(3N+z+z_1)}{N^2(N+z+z_1)}\right] +$$
$$\frac{3(y-y_1)^2}{M^5} - \frac{6z_1}{N^5}\cdot$$
$$\left.\left[3z_1 - (3-2\mu)(z+z_1) + \frac{5(y-y_1)^2 z}{N^2}\right]\right\}$$
$$(3)$$

The additional stress in the z-axis is

$$\sigma_{zy}(x,y,z,x_1,y_1,z_1) = \frac{(y-y_1)}{8\pi(1-\mu)}\left\{\frac{-1+2\mu}{M^3} + \frac{1-2\mu}{N^3} + \right.$$
$$\frac{3(z-z_1)^2}{M^5} + \frac{3(3-4\mu)(z+z_1)^2}{N^5} - \frac{6z_1}{N^5} \quad (4)$$
$$\left.\left[z_1 + (1-2\mu)(z+z_1) + \frac{5z(z+z_1)^2}{N^2}\right]\right\}$$

The unloading effect of the excavation is simplified as the horizontal load distributed on the side wall of the foundation pit with load direction inside to the pit. The distributed load can be calculated by

$$p = \beta K_0 \gamma z \quad (5)$$

where p is the unloading of the side wall of the foundation pit (kN/m²); γ is the unit weight of the soil (kN/m³)，which can be the weighted average of the excavated soils if multilayered; K_0 is the coefficient of earth pressure at rest; β is the stress releasing coefficient of the side wall. The unloading of the side walls can be considered as the difference between the lateral load on the retaining structure after excavation and the horizontal static earth pressure in the initial state. Zhou et al.[14] reported that the stress releasing of the side walls will be balanced by the support system, i.e. the side walls are not unloaded, $\beta = 0$. However, the actual foundation pit retaining structure will be displaced, and the side walls will have corresponding unloading effects. Especially for tunnels close to the foundation pit, the unloading position is relatively close, and the unloading effect near the side wall is the most important influencing factor and cannot be ignored. Zhang et al.[10] directly took the total static earth pressure as unloading, that is, $\beta = 1$. That the supporting structure of the foundation pit can bear earth pressure is not taken into account by doing so, which is not reasonable for internal supporting structures with strong stiffness. In reality, the quantity of the unloading is affected by various factors such as the geological conditions, the envelope structure, and the construction technology level, etc. This paper temporarily takes $\beta = 50\%$ in all case studies, and factor sensitivity analysis according to different β values will be conducted in Section 4.

Taking the micro unit ($B/2$，ζ，η) of the side wall of the foundation pit①, and calculating the integrals according to Eqs.(1), (2) and (5), the additional stresses along the x- and z-axes of the soil outside the tunnel lining caused by the unloading of the side wall ① are

$$\sigma_{ax1}(z,l) = $$
$$-\beta K_0 \gamma \int_0^d \int_{-L/2}^{L/2} \eta \sigma_{xx}(a-D/2,l,z,B/2,\zeta,\eta)\mathrm{d}\zeta\mathrm{d}\eta \quad (6)$$

$$\sigma_{az1}(x,l) = $$
$$-\beta K_0 \gamma \int_0^d \int_{-L/2}^{L/2} \eta \sigma_{zx}(x,l,h-D/2,B/2,\zeta,\eta)\mathrm{d}\zeta\mathrm{d}\eta \quad (7)$$

Taking the micro unit (ξ，$-L/2$，η)of the side wall of the foundation pit with the number ②, and calculating the integrals according to Eqs. (3), (4) and (5), the additional stresses along the x-axis and z-axis of the soil outside the tunnel lining caused by the unloading of the side wall ② are

$$\sigma_{ax2}(z,l) = $$
$$\beta K_0 \gamma \int_0^d \int_{-B/2}^{B/2} \eta \sigma_{xy}(a-D/2,l,z,\xi,-L/2,\eta)\mathrm{d}\xi\mathrm{d}\eta \quad (8)$$

$$\sigma_{az2}(x,l) = $$
$$\beta K_0 \gamma \int_0^d \int_{-B/2}^{B/2} \eta \sigma_{zy}(x,l,h-D/2,\xi,-L/2,\eta)\mathrm{d}\xi\mathrm{d}\eta \quad (9)$$

Similarly, the additional stresses along the x- and z-axes of the soil outside the tunnel lining caused by the side wall ④ unloading are respectively

$$\sigma_{ax4}(z,l) = $$
$$-\beta K_0 \gamma \int_0^d \int_{-B/2}^{B/2} \eta \sigma_{xy}(a-D/2,l,z,\xi,L/2,\eta)\mathrm{d}\xi\mathrm{d}\eta \quad (10)$$

$$\sigma_{az4}(x,l) = $$
$$-\beta K_0 \gamma \int_0^d \int_{-B/2}^{B/2} \eta \sigma_{zy}(x,l,h-D/2,\xi,L/2,\eta)\mathrm{d}\xi\mathrm{d}\eta \quad (11)$$

By superimposing the additional stresses caused by the unloading effect of the three side walls of the foundation pit, the surcharge load distributions along the x- and z-axes of the nearby tunnel caused by the excavation of the foundation pit are

$$p_{\mathrm{ax}}(z,l) = \sigma_{\mathrm{ax1}}(z,l) + \sigma_{\mathrm{ax2}}(z,l) + \sigma_{\mathrm{ax4}}(z,l) \tag{12}$$

$$p_{\mathrm{az}}(x,l) = \sigma_{\mathrm{az1}}(x,l) + \sigma_{\mathrm{az2}}(x,l) + \sigma_{\mathrm{az4}}(x,l) \tag{13}$$

2.2.2 Redistribution of additional confining pressure by tunnel displacement

Excavation of the foundation pit will cause surcharge loads on the tunnel, and the balance condition of the confining pressures acting on the tunnel will be broken. The tunnel is displaced under combined forces. During the process of coordinated deformation of the tunnel and the soil, the confining pressure of the tunnel will be redistributed until the forces are balanced, and the tunnel deformation tends to be stable. Actually, this is a simultaneous overall process. In order to facilitate calculation, this paper divides this process into three stages. In the first stage, as shown in Fig.2(a), the excavation side of the foundation pit of the tunnel is subjected to horizontal and vertical surcharge loads p_{ax} and p_{az}, respectively. Because the confining pressure of the tunnel is unbalanced due to the effect of the surcharge load, the tunnel will be displaced to the smaller side of the confining pressure, and the tunnel axis will undergo longitudinal deformation. The cross-section has an overall displacement along the direction of the surcharge load. As shown in Fig.2(b), during the cross-section displacement in the second stage, the soil on the side of the displacement direction is compressed, and the confining pressure is increased. The horizontal and vertical additions load increments are $\Delta p'_{\mathrm{ax}}$ and $\Delta p'_{\mathrm{az}}$ respectively. The soil stress on the opposite side of the displacement is released, causing the confining pressure to reduce, and the horizontal and vertical surcharge loads to increase by $\Delta p''_{\mathrm{ax}}$ and $\Delta p''_{\mathrm{az}}$, respectively. Because the cross-section of the tunnel moves as a whole and the displacement values on the two sides are the same, the surcharge load increments on the two sides of the tunnel can be considered equal, i.e. $\Delta p'_{\mathrm{ax}} = \Delta p''_{\mathrm{ax}}$, $\Delta p'_{\mathrm{az}} = \Delta p''_{\mathrm{az}}$. The surcharge load increments in all directions can be simplified into rectangular uniform loads. In the third stage, when the deformation of the tunnel is stable, as shown in Fig.2 (c), the horizontal surcharge loads on both sides are p'_{ax} and p''_{ax}, and the vertical surcharge loads on the two sides are p'_{az} and p''_{az}. When the deformation of the tunnel is stable, the surcharge load satisfies the following equations:

$$\left.\begin{array}{l} p'_{\mathrm{ax}}(z,l) = p_{\mathrm{ax}}(z,l) - \Delta p'_{\mathrm{ax}} \\ p'_{\mathrm{az}}(x,l) = p_{\mathrm{az}}(x,l) - \Delta p'_{\mathrm{az}} \end{array}\right\} \tag{14}$$

$$\left.\begin{array}{l} p''_{\mathrm{ax}}(z,l) = \Delta p''_{\mathrm{ax}} \\ p''_{\mathrm{az}}(x,l) = \Delta p''_{\mathrm{az}} \end{array}\right\} \tag{15}$$

Meanwhile, the segment rings of the cross section are misaligned to the adjacent ones, and are subjected to the shear constraint of the adjacent ones. Let the shear force in the x-axis be F_{sx}, and the shear force in the y-axis be F_{sy}. In the end, all

the forces reached equilibrium in the horizontal and vertical directions, and the cross-section displacement of the tunnel reached stability. The following equations can be obtained:

$$\int_{h-D/2}^{h+D/2} p'_{\mathrm{ax}}(z,l)\mathrm{d}z = \int_{h-D/2}^{h+D/2} p''_{\mathrm{ax}}(z,l)\mathrm{d}z + F_{\mathrm{sx}}(l) \tag{16}$$

$$\int_{h-D/2}^{h+D/2} p'_{\mathrm{az}}(x,l)\mathrm{d}x = \int_{h-D/2}^{h+D/2} p''_{\mathrm{az}}(x,l)\mathrm{d}x + F_{\mathrm{sz}}(l) \tag{17}$$

(a) The first stage　　　　　　(b) The second stage

(c) The third stage
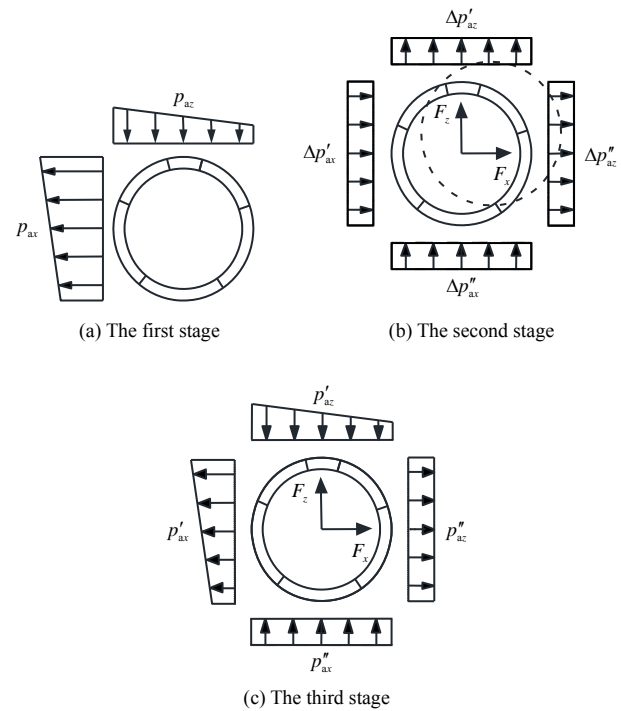
Fig.2　Schematic diagram of tunnel confining pressure redistribution with additional load of excavation

Substituting Eqs. (14) and (15) into Eqs. (16) and (17), respectively, we have

$$\int_{h-D/2}^{h+D/2} p_{\mathrm{ax}}(z,l)\mathrm{d}z = \int_{h-D/2}^{h+D/2} \Delta p'_{\mathrm{ax}}\mathrm{d}z + \int_{h-D/2}^{h+D/2} \Delta p''_{\mathrm{ax}}\mathrm{d}z + F_{\mathrm{sx}}(l) \tag{18}$$

$$\int_{h-D/2}^{h+D/2} p_{\mathrm{az}}(x,l)\mathrm{d}x = \int_{h-D/2}^{h+D/2} \Delta p'_{\mathrm{az}}\mathrm{d}x + \int_{h-D/2}^{h+D/2} \Delta p''_{\mathrm{az}}\mathrm{d}x + F_{\mathrm{sz}}(l) \tag{19}$$

Since the surcharge load increments in all directions are simplified to a rectangular uniform load, and $\Delta p'_{\mathrm{ax}} = \Delta p''_{\mathrm{ax}} h$, $\Delta p'_{\mathrm{az}} = \Delta p''_{\mathrm{az}}$, according to Eqs. (18) and (19)

$$\Delta p'_{\mathrm{ax}} = \Delta p''_{\mathrm{ax}} = \frac{\int_{h-D/2}^{h+D/2} p_{\mathrm{ax}}(z,l)\mathrm{d}z - F_{\mathrm{sx}}(l)}{2D} \tag{20}$$

$$\Delta p'_{\mathrm{az}} = \Delta p''_{\mathrm{az}} = \frac{\int_{h-D/2}^{h+D/2} p_{\mathrm{az}}(x,l)\mathrm{d}x - F_{\mathrm{sz}}(l)}{2D} \tag{21}$$

Substituting Eqs. (20) and (21) into Eqs. (14) and (15) gives

$$\left.\begin{array}{l} p'_{\mathrm{ax}}(z,l) = p_{\mathrm{ax}}(z,l) - \dfrac{\int_{h-D/2}^{h+D/2} p_{\mathrm{ax}}(z,l)\mathrm{d}z - F_{\mathrm{sx}}(l)}{2D} \\[4mm] p'_{\mathrm{az}}(x,l) = p_{\mathrm{az}}(x,l) - \dfrac{\int_{h-D/2}^{h+D/2} p_{\mathrm{az}}(x,l)\mathrm{d}x - F_{\mathrm{sz}}(l)}{2D} \end{array}\right\} \tag{22}$$

$$
\left.\begin{aligned}
p_{ax}''(z,l) &= \dfrac{\int_{h-D/2}^{h+D/2} p_{ax}(z,l)\mathrm{d}z - F_{sx}(l)}{2D} \\[2mm]
p_{az}''(x,l) &= \dfrac{\int_{h-D/2}^{h+D/2} p_{az}(x,l)\mathrm{d}x - F_{sz}(l)}{2D}
\end{aligned}\right\} \tag{23}
$$

At the same time, the additional confining pressure of the tunnel lining after deformation stabilization can be obtained according to the distribution of the surcharge load as

$$
p_{ar}(\theta,l)=\begin{cases}
p_{ax}''(h-\dfrac{D\cos\theta}{2},l)\sin\theta+ \\
p_{az}'(a+\dfrac{D\sin\theta}{2},l)\cos\theta,\ \ 0\leqslant\theta<\dfrac{\pi}{2} \\[1mm]
p_{ax}''(h-\dfrac{D\cos\theta}{2},l)\sin\theta+ \\
p_{az}''(a+\dfrac{D\sin\theta}{2},l)\cos\theta,\ \ \dfrac{\pi}{2}\leqslant\theta<\pi \\[1mm]
p_{ax}'(h-\dfrac{D\cos\theta}{2},l)\sin\theta+ \\
p_{az}''(a+\dfrac{D\sin\theta}{2},l)\cos\theta,\ \ \pi\leqslant\theta<\dfrac{3\pi}{2} \\[1mm]
p_{ax}'(h-\dfrac{D\cos\theta}{2},l)\sin\theta+ \\
p_{az}'(a+\dfrac{D\sin\theta}{2},l)\cos\theta,\ \ \dfrac{3\pi}{2}\leqslant\theta<2\pi
\end{cases} \tag{24}
$$

According to relevant measurement data[1, 15], it can be found that the displacement of the tunnel is normally distributed along the tunnel axis, and the displacement value of the tunnel corresponding to the excavation interval is the largest. According to the research results of the staggered deformation model of the shield tunnel[14], it is found that the segment at the position with the largest longitudinal displacement is basically free of inter-ring stagger. That is, in theory, at the excavation center ($y=0$) of the foundation pit corresponding to the tunnel position ($l=0$), the overall displacement of the segment ring is the largest, and the displacement amount is 0. There is no shear binding force caused by the misalignment between the rings, i.e. $F_{sx}(0)=F_{sy}(0)=0$. Substituting into Eqs. (22) and (23), the distribution of the surcharge load on the section where the longitudinal displacement is maximum after the tunnel deformation is

$$
\left.\begin{aligned}
p_{ax}'(z,0) &= p_{ax}(z,0) - \dfrac{\int_{h-D/2}^{h+D/2} p_{ax}(z,0)\mathrm{d}z}{2D} \\[2mm]
p_{az}'(x,0) &= p_{az}(x,0) - \dfrac{\int_{h-D/2}^{h+D/2} p_{az}(x,0)\mathrm{d}x}{2D}
\end{aligned}\right\} \tag{25}
$$

$$
\left.\begin{aligned}
p_{ax}''(z,0) &= \dfrac{\int_{h-D/2}^{h+D/2} p_{ax}(z,0)\mathrm{d}z}{2D} \\[2mm]
p_{az}''(x,0) &= \dfrac{\int_{h-D/2}^{h+D/2} p_{az}(x,0)\mathrm{d}x}{2D}
\end{aligned}\right\} \tag{26}
$$

2.3 Calculation of initial load and internal force

At present, the design and calculation of shield tunnel linings in soft soil are mainly based on the load–structure method. Among them, the modified routine method (MRM) is widely used because of its simplicity of force equilibrium and clarity of calculation procedure. Both the routine method and

the modified routine method assume the segmental rings to have uniform stiffness. However, the modified routine method additionally introduces the effective bending stiffness ratio and bending moment increase rate which would reduce the stiffness of the lining ring in order to reflect the influence of segment joints on the lining structure.

The tunnel is subject to initial balance loads from water pressure and earth pressure, respectively, before the construction of the foundation pit beside the tunnel. The load combinations of initial conditions considered in this study are shown in Fig.3(a), where the initial load combination consists of the self-weight of the lining (g), the vertical earth pressure from overlying soil (q), the lateral earth pressure(p_e), the hydro-static water pressure (p_w), the bottom reaction force (q_R), and the lateral soil resistance caused by deformation of the segment ring under various loads(p_k). After construction of the tunnel, the additional confining pressures of the tunnel lining with stabilized deformation as computed by the method in section 2.2 are shown in Fig.3 (b).

In this paper, based on the confining pressure of the initial load, the above-mentioned methods are combined to calculate the additional cross-section confining pressure caused by foundation pit excavation. The Shield Tunnel Design and Analysis Software of GeoFBA is used to calculate the change of its internal force using modified routine methods to study the effect of foundation pit excavation on the stress of nearby tunnels.

(a) Initial load combination

(b) Surcharge load combination
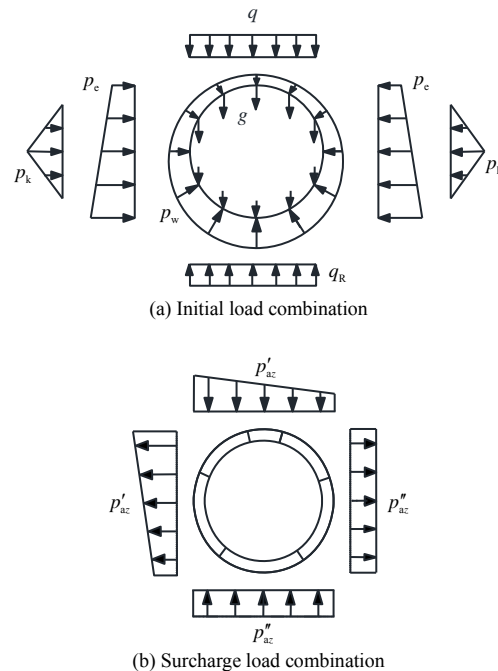
Fig.3　Schematic diagram of initial load combination and additional load combination

3　Case studies

3.1　Description of the engineering problem

This paper will take a deep foundation pit project beside the shield tunnel of Hangzhou Metro Line 2 as an actual case study. The project is located near the intersection of Shixin middle road and Jincheng road in Xiaoshan distinct. Excavation

dimensions of the foundation pit beside the tunnel are $L =$ 68 m, $B = 72$ m, excavation depth $d = 15.8$ m, and the diaphragm wall penetrates 37.2 m below the ground. Buried depth of tunnel $h = 14.3$ m, the minimum clear distance between the sideline of the foundation pit retaining structure and the tunnel $s = 9.5$ m. Shield tunnel lining outer diameter $D = 6.2$ m, using C50 concrete segment, thickness $t = 0.35$ m, Ring width $D_t = 1.2$ m. During the construction process, there is no dewatering outside the pit near the side of the subway tunnel, and the groundwater level is about 1.02 m. As the fluctuation of water level during the excavation of the foundation pit is small, the calculation does not consider the change of the groundwater level. The soil layer distribution and corresponding parameters near the side of the subway tunnel are shown in Table 1.

Table 1   Soil layer distribution and physical and mechanical parameters

Layer number	Geotechnical type	Thickness / m	Gravity density γ / (kN/m³)	Saturated gravity density γ / (kN/m³)	Cohesion c / kPa	Friction angle φ / (°)
①–2	Miscellaneous fill	2.2	18.7	19.0	10.0	8.0
②–1	Silt clay	1.7	19.2	19.3	25.6	10.0
③–1	Sandy silt	4.0	18.3	18.6	3.1	25.5
③–2	Sandy silt	2.8	19.2	19.4	3.2	25.8
③–3	Silt sand	4.3	19.7	19.9	3.7	26.0
③–3S	Sandy silt	2.0	19.0	19.2	3.5	25.6
④–1	Muddy silty clay	13.3	17.2	17.4	19.8	8.2

3.2   Calculation results

On the cross section of the tunnel, the surcharge loads caused by foundation pit excavation as proposed in this paper is superimposed on the confining pressure of the initial load. The modified routine method is used to calculate the change of internal force in order to study the influence of excavation on the lateral tunnel forces.

Figure 4 shows the calculated values of the tunnel confining pressure before and after the excavation in this case. The confining pressure of the entire circumference of the tunnel before the excavation of the foundation pit is distributed in a "bell shape", and the confining pressure in the lower portion is greater than that in the upper portion. This is mainly due to the increase in soil and water pressures on both sides with increasing depth. The above apex is 0°, and the angle increases clockwise. The confining pressure between 0° and 90° is small, about 200 kPa. The confining pressure increases rapidly from 90° to 120°, and reaches the maximum value of about 244.96 kPa at 150°. The confining pressure at the bottom of the tunnel is 234.92 kPa. Before excavation of the foundation pit, the confining pressure on the left and right sides of the tunnel is symmetrically distributed. When the foundation pit is excavated, the confining pressures on both sides of the tunnel decrease, and the confining pressures on the top and bottom increase slightly.

Figure 5 shows the additional confining pressure of the nearby tunnel caused by the excavation of the foundation pit, i.e., the change of confining pressure, with negative value

denoting the reduction. It is found that only the confining pressures at the top and the bottom tend to increase slightly by 0.96 kPa. Confining pressure reduction on the right side of the tunnel is greater than that on the left side of the tunnel. This is consistent with the confining pressure distribution as obtained from the laboratory model test results[16]. The maximum reduction in confining pressure in this case is 10.03 kPa, which is at 285°. The absolute value of the additional confining pressure on the excavation side of the tunnel is greater than that of the additional confining pressure on the lower part. In other words, the amount of confining pressure reduction at the upper part of the tunnel is bigger than that of the lower part, both are on the excavation side of the foundation pit.
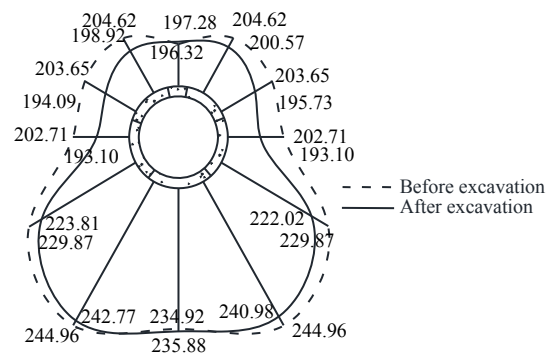
Fig.4   Comparison of confining pressures before and after excavation of foundation pit (unit: kPa)
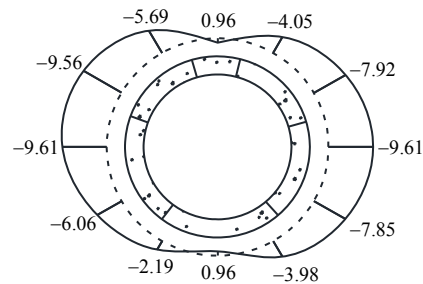
Fig.5   Additional confining pressure on shield tunnel caused by nearby excavation (unit: kPa)

The internal forces of the tunnel lining rings before and after the excavation are analyzed using the modified routine method. Figure 6 are comparisons of the bending moments, shear and axial forces. Table 2 shows the comparison of the extreme values of the internal forces before and after the excavation. As shown in Fig.6(a), the distribution of the bending moments before and after the excavation of the foundation pit is basically the same. The inside of the lining at the top and bottom of the tunnel is in tension with a positive bending moment, and the outside of the lining haunch is in tension with a negative bending moment. The negative moment area is symmetrically distributed. The range of the positive bending moment of the vault is about 90°. The range of the positive bending moment of the vault is slightly smaller than that of the arch bottom, but the maximum bending moment is larger than that of the arch bottom. According to Table 2, before

the excavation of the foundation pit, the maximum positive bending moment 77.07 kN m appears at the position of 0° and the maximum negative bending moment of − 58.21 kN・m appears at the position 77.73°. Both positive and negative moments after the excavation of the foundation pit are greater than those before the excavation. The maximum positive bending moment is 108.39 kN・m, which is also located at 0° and has increased by 40.64% compared with that before excavation. The maximum negative bending moment is -86.45 kN m, which is located at the excavation side of the foundation pit at 278.18° and has an increase of 48.51% compared with that before the excavation.

As shown in Fig.6(b), there are zero points of shear forces at the positions near 0°, 80°, 18°, and 280° on the cross section of the tunnel. The upper half of the lining has a higher shear force than the lower half. The positive and negative shear forces after the excavation of the foundation pit are greater than those before the excavation. According to Table 2, before the

excavation, the maximum absolute values of the positive and negative shear forces are both 43.29 kN, which are respectively at the positions of 323.18° and 36.82°. After the excavation of the foundation pit, the position of the maximum positive and minimum negative shear forces do not change, and the absolute value of the shear force increases to 59.54 kN, which is 37.54% larger than those before the excavation.

As shown in Fig.6(c), the axial force of the tunnel lining is larger at the haunch. Also, the axial force at the top is smaller than that at the bottom, and the axial force distribution is symmetrical on the whole. According to Table 2, it can be seen that the maximum value of the axial forces before and after the excavation of the foundation pit tend to slightly increase, and the position of the maximum axial force moves slightly from 98.18° before excavation to 94.09°. The axial force at the position of 0° before the excavation is 487.29 kN. After the excavation, the axial force reduces to 454.64 kN, i.e., decrease by 6.7%.

(a) Bending moment (unit: kN・m)　　(b) Shear force (unit: kN)　　(c) Axial force (unit: kN)
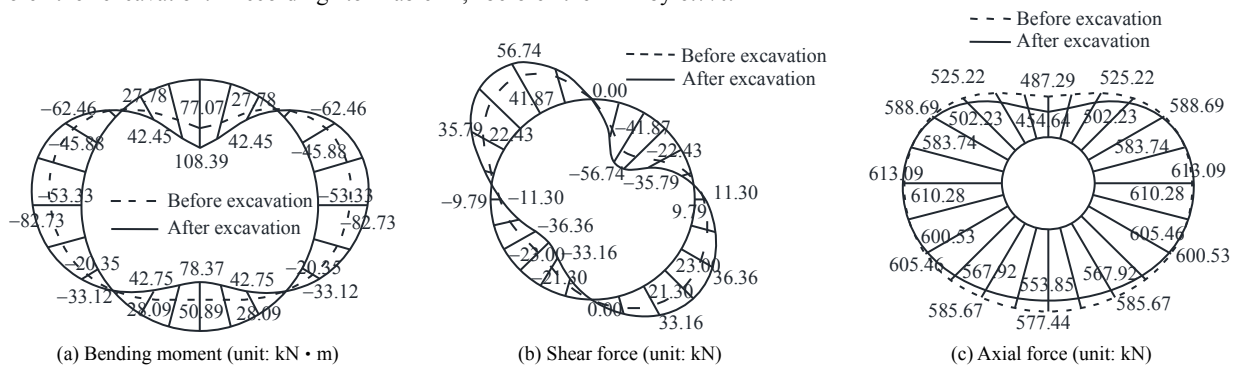
Fig.6 Comparison of tunnel lining internal forces before and after excavation

Table 2　Extreme values of internal forces of tunnel lining and their location before and after excavation

Condition	Maximum bending moment		Minimum bending moment		Maximum shear force		Minimum shear force		Maximum axial force		Minimum axial force	
	Value / (kN・m/m)	Position / (°)	Value / (kN・m/m)	Position / (°)	Value / (kN・m⁻¹)	Position / (°)	Value / (kN・m⁻¹)	Position / (°)	Value / (kN・m⁻¹)	Position / (°)	Value / (kN・m⁻¹)	Position / (°)
Before excavation	77.07	0.00	−58.21	77.73	43.29	323.18	−43.29	36.82	611.38	98.18	487.29	0.00
After excavation	108.39	0.00	−86.45	278.18	59.54	323.18	−59.54	36.82	613.60	94.09	454.64	0.00

4　Parametric analysis of influencing factors

4.1　Effect of stress releasing coefficient β of the foundation pit side wall on tunnel stress

In the literature, most studies did not consider the unloading effect of the side wall[14], but the actual foundation pit retaining structure will be displaced. Thus, there are corresponding unloading effects at the side walls of the excavated foundation pit. Particularly the unloading effects of the adjacent side walls of the foundation pit will affect the nearby tunnels and cannot be ignored[12]. In the study of the unloading effect of the side wall of the foundation pit, the total static earth pressure is taken as the unloading[10]. That means the stress release coefficient of the side wall of the foundation pit is $\beta = 100\%$. There are also studies that take $\beta = 25\%$ based on the results of finite element simulations[17]. In this paper, in order to study the influence of

the value of the stress releasing coefficient β on the tunnel force, $\beta = 25\%$, $\beta = 50\%$, $\beta = 75\%$ and $\beta = 100\%$ are taken respectively. The additional confining pressure of the tunnel caused by the excavation of the foundation pit is calculated, as shown in Fig.7.

It was concluded that the additional confining pressures are only positive at the top and bottom, and the values are small, the other ranges are mainly negative. That is, the excavation of the foundation pit mainly reduces the confining pressure of the tunnel, and as β increases, the reduction amount of the confining pressure of the foundation pit increases. The maximum absolute value of the additional confining pressure of different β all appears at 285 °, i.e., the location above the haunch of the lining in the excavation side of the foundation pit. When $\beta = 25\%$, $\beta = 50\%$, $\beta = 75\%$ and $\beta = 100\%$, the maximum absolute values of additional confining pressures

correspond to 5.01, 10.03, 15.04, 20.06 kPa, which respectively account for 2.45%, 4.91%, 7.36% and 9.81% of the initial confining pressure at the corresponding positions before the excavation of the foundation pit.
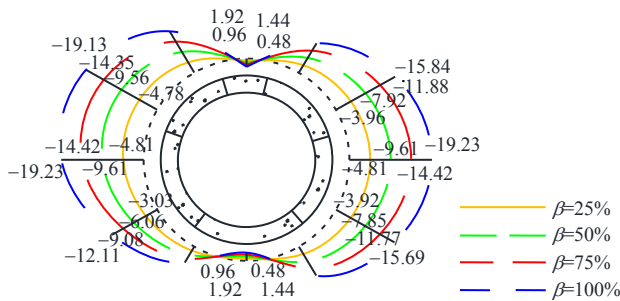
Fig.7   Additional confining pressures caused by excavation with different values of β (unit: kPa)

Figure 8 shows comparison of the additional bending moments of the tunnel lining when $\beta = 25\%$, $\beta = 50\%$, $\beta = 75\%$ and $\beta = 100\%$, respectively. Except for the additional bending moments of 45°, 135°, 225° and 315°, the positive and negative bending moments at other locations increase uniformly with the increase of β value, and the additional positive bending moments are all maximum at 0°. At $\beta = 25\%$, $\beta = 50\%$, $\beta = 75\%$ and $\beta = 100\%$, the additional bending moments are 15.66, 31.32, 46.98, 62.64 kN•m, which account for 20.32%, 40.64%, 60.96%, and 81.28% of the initial bending moments at the corresponding positions before the excavation. The maximum additional negative bending moments at the haunch are − 14.70, − 29.4, − 44.1 and − 58.8 kN•m，respectively, accounting for 27.56%, 55.13%, 82.69%, and 110.26% of the initial bending moments at the corresponding positions before the excavation.
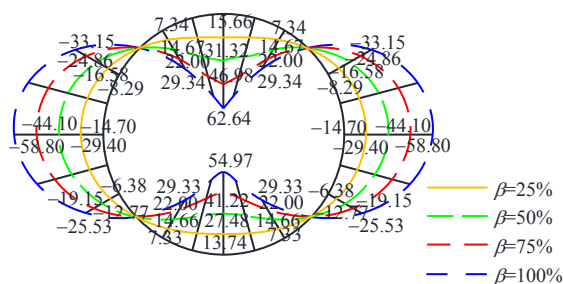
Fig.8   Additional moments caused by excavation with different values of β (unit: kN•m)

It can be seen that the change in the confining pressure caused by the excavation of the foundation pit is not large. When the stress releasing coefficient is set to $\beta = 100\%$, the maximum additional confining pressure only accounts for less than 10% of the initial confining pressure. However, the bending moment response of the lining with changing confining pressure is more obvious, especially for the negative bending moment at the haunch. When the stress release coefficient is only 25%, the additional negative bending moment reaches 27.56% of the initial confining pressure. When the stress

release coefficient increases to $\beta = 100\%$, the negative bending moment increases even more than 100%. According to the results, the excavation of the foundation pit mainly reduces the confining pressure on both sides of the tunnel, and the vertical confining pressure increases slightly. At the same time, the excavation of the foundation pit exacerbates the horizontal stretching and vertical compression of the tunnel lining[18], resulting in a large increase in internal force.

4.2   Influence of excavation of foundation pits on the stress of tunnels with different buried depths

Next, let us take the working conditions in Section 3.1, and only change the buried depth of the shield tunnel. The buried depths of the tunnel are taken as $h = 1/2d$, $h = d$ and $h = 3/2d$, and d is the excavation depth of the foundation pit. In the example, $d = 15.8$m. As shown in Fig.9, the additional confining pressure of the tunnel caused by the excavation of the foundation pit is obtained. When $h = 1/2d$ and $h = d$, the distributions of the additional confining pressure are different, but their values are close. When $h = 1/2d$, the maximum absolute confining pressure is 10.32 kPa, which is located at 255 ° of the tunnel lining, i.e. the lower position of the tunnel lining haunch on the excavation side of the foundation pit. When $h = d$, the maximum absolute confining pressure is 9.52 kPa, which is located at 285 ° of the tunnel lining, i.e. the upper position of the tunnel lining haunch on the excavation side. When the burial depth is greater than the excavation depth, $h = 3/2d$, the absolute values of the additional confining pressures on both sides of the tunnel will be significantly reduced. The maximum absolute confining pressure is 5.05 kPa, which is located at 315 ° of the tunnel lining, i.e. the position of the tunnel lining on the excavation side near the vault.
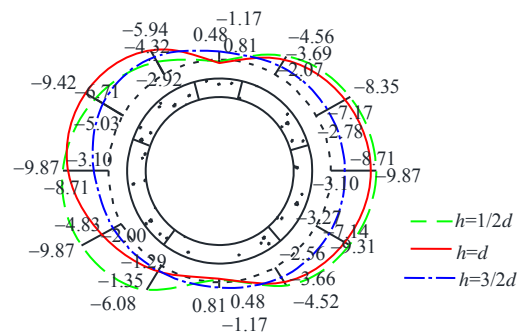
Fig.9   Additional confining pressures of shield tunnels with different buried depths caused by excavation(unit: kPa)

Figure 10 shows the comparison of the additional bending moments of the tunnel burial depths of $h = 1/2d$, $h = d$ and $h = 3/2d$, respectively. When $h = 1/2d$ and $h = d$, the distribution of additional bending moments is close. The maximum additional positive bending moments are located at 0 °, which are 30.47 and 28.94 kN • m respectively. At $h = 1/2d$, the maximum additional negative moment is − 27.87   kN•m, which is located at 265 °. At $h = d$, the maximum additional negative bending moment is − 26.66 kN•m, and the position is slightly higher, which is about 275 °. It can also be seen from Fig.10 that when the burial depth is greater

than the excavation depth, $h = 3/2d$, the positive and negative additional bending moments are significantly reduced and the distribution is more uniform. The maximum additional positive and negative bending moments are 6.71 and -5.7 kN•m respectively, located at 0° and 280°.

According to the analysis results of Fig. 9 and Fig. 10, it can be found that the surcharge load caused by the excavation of the foundation pit is larger for the tunnel with a shallow burial depth, and the bending moment changes significantly. The change of confining pressure of a tunnel with a large burial depth is less and the internal force response is not obvious. This is somewhat consistent with the results obtained from the model test[16]. Therefore, shield tunnels with shallower burial depth are more sensitive to the impact of side pit excavations. Tunnels with large burial depth, especially those with a burial depth greater than the excavation depth of the foundation pit, will significantly reduce the impact of the side foundation pit excavation.
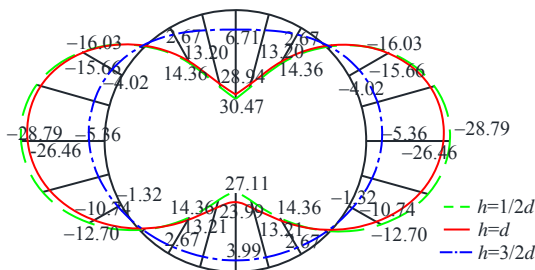
Fig.10   Additional moments of shield tunnels with different buried depths caused by excavation(unit: kN•m)

4.3   Impact of excavation of foundation pit on nearby tunnels at different distances

Finally, let us take the working conditions in Section 3.1, and only change the clear distance between the sideline of the foundation pit and the nearby tunnel. The clear distances between the side line of the foundation pit and the nearby tunnels are $s = 1/3d$, $s = 2/3d$, and $s = d$, respectively, and the excavation depth of the foundation pit is $d = 15.8$ m. The additional confining pressure of the tunnel caused by the excavation is obtained. As shown in Fig.11, as the clear distance between the foundation pit and the nearby tunnel increases, the additional confining pressure of the tunnel caused by the excavation of the foundation pit decreases. The absolute value of the additional confining pressure at $s = d$ is smaller than that at $s = 2/3d$ in all locations, but the difference is small, which is mainly reflected on the tunnel close to the foundation pit, and the overall distribution is basically the same. When the clear distance between the foundation pit and the tunnel is further reduced to $s = 1/3d$, the value of the additional confining pressure at the upper part in the excavation side of the foundation pit increase significantly, mainly in the range of 270° to 360°. When $s = 1/3d$, the absolute maximum confining pressure is 14.13 kPa, which accounts for 6.94% of the initial confining pressure at the corresponding position before the foundation pit excavation.
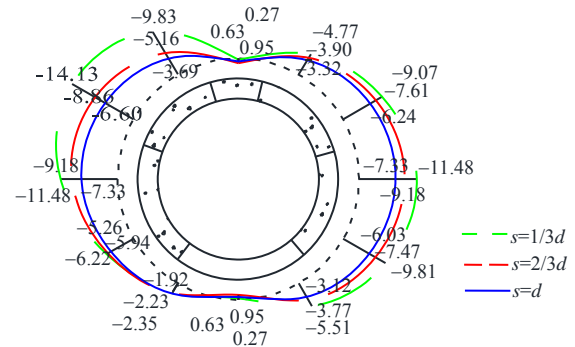
Fig.11 Additional confining pressures of shield tunnels with different distances caused by excavation (unit: kPa)

Figure 12 compares the additional bending moments when the clear distances between the foundation pit and the tunnel are $s = 1/3d$, $s = 2/3d$ and $s = d$ respectively, which are similar to the model test results [16]. As the distance between the tunnel and the foundation pit increases, the additional positive and negative bending moments of the tunnel lining caused by the excavation decrease sequentially. When the clear distances are $s = 1/3d$, $s = 2/3d$ and $s = d$ respectively, the maximum additional positive bending moments remain at 0°, which are 36.50, 29.8, and 22.96 kN•m, accounting for 47.36%, 38.67%, and 29.79% of the initial bending moment before the excavation. When the distance between the foundation pit and the tunnel is small, $s = 1/3d$, the maximum additional negative bending moment is at 275°, which is located on the upper side of the lining haunch in the excavation side. When $s = 2/3d$ and $s = d$, the maximum additional negative bending moment is at 270°, which is exactly at the position of the lining haunch in the excavation side.
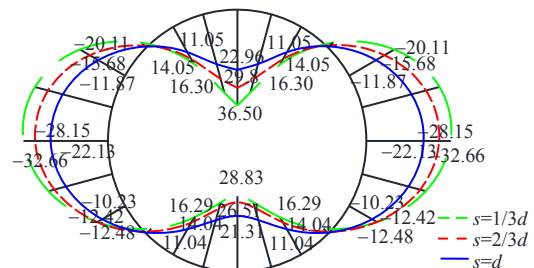
Fig.12   Additional moments of shield tunnels with different distances caused by excavation (unit: kN•m)

5   Conclusions

(1) Before the excavation of the foundation pit, the confining pressure around the tunnel is distributed symmetrically with a "bell shape". After the excavation, the confining pressures on both sides of the tunnel cross section decrease, the confining pressure on the excavation side of the foundation pit decreases more than that on the other side, and the confining pressure near the haunch decreases more significantly.

(2) Excavation of the foundation pit will increase the positive and negative bending moment values and the positive

and negative shear force values of the nearby tunnels, and reduce the axial force of the arch top and bottom. With the increase of the stress releasing coefficient of the foundation pit side wall, the absolute values of the additional confining pressure and the additional bending moment of the shield tunnel lining increase significantly. The response of the bending moment to the unloading of the foundation pit is more obvious than to the change of confining pressure.

(3) Shield tunnels with shallower burial depth are more sensitive to the impact of side pit excavations. Tunnels with large burial depth, especially those with a burial depth greater than the excavation depth of the foundation pit, will be less sensitive to be affected by the side foundation pit excavation. With the increase of the clear distance between the foundation pit and the nearby tunnel, the impact of the excavation on the tunnel will be further reduced.

The distribution of additional confining pressures and the influence of factors obtained in this paper are consistent with the results of existing laboratory model tests, which verifies the reliability of this method. When calculating the surcharge load of the tunnel caused by the excavation of the foundation pit, the load distribution and the properties of the soil layer are simplified in this paper, and further discussion is needed in the subsequent research. Although the modified routine method has the advantages of simplicity and practicality, the calculation accuracy of the internal force is poor, and the mechanical characteristics of the segment joint need to be considered for further refinement.

References

[1]   WEI Gang, LI Jing, XUAN Hai-li, et al. Monitoring data analysis on the influence of large deep foundation pit excavation on nearby metro shield tunnel[J]. Journal of Railway Science and Engineering, 2018, 15(3): 718–726.

[2]   ZHANG Zhi-guo, XI Xiao-guang, WU Ling. Numerical simulation and site monitoring analysis of influence of division excavation of foundation pit on adjacent large-diameter river-crossing tunnel[J]. Tunnel Construction, 2018, 38(9): 1480–1488.

[3]   YAN Jing-ya, WANG Ru-lu. Cause analysis and typical characteristics of settlement and transverse convergence deformation of metro tunnel in soft ground in Shanghai[J]. Journal of Natural Disasters, 2018, 27(4): 178–187.

[4]   Ministry of Housing and Urban-Rural Development of the Peoples Republic of China. GB 50911－2013 Code for monitoring measurement of urban rail transit engineering[S]. Beijing: China Architecture & Building Press, 2013.

[5]   WANG Li-feng, PANG Jin, XU Yun-fu, et al. Influence of foundation pit excavation on adjacent metro tunnels[J]. Rock and Soil Mechanics, 2016, 37(7): 2004–2010.

[6]   GUO Peng-fei, YANG Long-cai, ZHOU Shun-hua, et al. Measurement data analyses of heave deformation of shield tunnels due to overlying pit excavation[J]. Rock and Soil Mechanics, 2016, 37(Suppl.2): 613–621.

[7]   ZHENG Gang, DU Yi-ming, DIAO Yu, et al. Influenced zones for deformation of existing tunnels adjacent to excavations[J]. Chinese Journal of Geotechnical Engineering, 2016, 38(4): 599–612.

[8]   HU Hai-ying, ZHANG Yu-cheng, YANG Guang-hua, et al. Measurement and numerical analysis of effect of excavation of foundation pits on metro tunnels[J]. Chinese Journal of Geotechnical Engineering, 2014, 36(Suppl.2): 431–439.

[9]   ZHOU Ze-lin, CHEN Shou-gen, TU Peng, et al. Coupling method for analyzing the influence on existing tunnel due to adjacent foundations pit excavation[J]. Rock and Soil Mechanics, 2018, 39(4): 1440–1449.

[10] ZHANG Zhi-guo, ZHANG Meng-xi, WANG Wei-dong. Two-stage method for analyzing effects on adjacent metro tunnels due to foundation pit excavation[J]. Rock and Soil Mechanics, 2011, 32(7): 2085–2092.

[11] LIANG Fa-yun, CHU Feng, SONG Zhu, et al. Centrifugal model test research on deformation behaviors of deep foundation pit adjacent to metro stations[J]. Rock and Soil Mechanics, 2012, 33(3): 657–664.

[12] WEI Gang, ZHAO Cheng-li. Calculation method of surcharge load caused by excavation of foundation pit adjacent to metro tunnel[J]. Chinese Journal of Rock Mechanics and Engineering, 2016, 35(Suppl.1): 3408–3417.

[13] MINDLIN R D. Force at a point in the interior of a semi-infinite solid[J]. Physics, 1936, 7(5): 195–201.

[14] ZHOU Shun-hua, HE Chao, XIAO Jun-hua. Energy method for calculating deformation of adjacent shield tunnels due to foundation pit excavation considering step between rings[J]. China Railway Science, 2016, 37(3): 53–60.

[15] WEI Gang. Measurement and analysis of impact of foundation pit excavation on below existed shield tunnels[J]. Rock and Soil Mechanics, 2013, 34(5): 1421–1428.

[16] HU Xin. Influence of foundation pit excavation under different conditions simulating by model test on existing tunnel[J]. Subgrade Engineering, 2015(6): 151–155.

[17] JIANG Zhao-hua, ZHANG Yong-xing. Calculation method of the influence of excavation on the longitudinal displacement of adjacent tunnel[J]. Journal of Civil, Architectrual & Environment Engineering, 2013, 35(1): 7–11, 39.

[18] WEI Gang, ZHAO Cheng-li. On calculation formula of existing metro tunnel displacements induced by adjacent foundation pit excavation[J]. Modern Tunnelling Technology, 2018, 55(1): 124–132.